Simulation and Design of Tentative Muon Source Based on CSNS

2012 Plasma Sci. Technol. 14 469

(http://iopscience.iop.org/1009-0630/14/6/07)

Plasma Science and Technology, Vol.14, No.6, Jun. 2012

Simulation and Design of Tentative Muon Source Based on CSNS*

XU Wenzhen (许文贞), LIU Yanfen (刘艳芬), YE Bangjiao (叶邦角)

Department of Modern Physics, University of Science and Technology of China, Hefei 230026, China

Abstract This paper presents a conceptual design for the first tentative surface muon source based on the proton beam provided by China Spallation Neutron Source (CSNS). We have calculated the optimal parameters of solid muon target, in which the method of Monte Carlo simulation is used to obtain the optimal muon beam parameters, such as beam fluence rate, momentum spread and phase space distribution. A simple muon transport beamline system was also designed, which could transport the muons emitted from the muon target into the experimental area, where positrons from muon decay in a test sample are detected by a spectrometer. The beam optics of this new beam line is also described.

Keywords: spallation neutron source, surface muon, muon production target, charged particle transport

PACS: *07.77.Ka, 29.27.Eg, 29.25.Pj*

DOI: 10.1088/1009-0630/14/6/07

1 Introduction

China Spallation Neutron Source (CSNS) [1] is a large accelerator-based scientific facility to provide a high intensity pulsed neutron source (2.0×10^{16} n/cm^{2}s) by 1.6 GeV protons bombarding solid tungsten target. The CSNS complex is to be operated at 25 Hz repetition rate with a proton beam power of 120 kW (Phase I). When successfully built, CSNS will provide an advanced platform for fundamental and applied research in China. Besides serving as spallation neutron source, CSNS can also be used as a potential multi-purpose particle source for more extended applications, such as proton beams application, muon source, etc. Furthermore, the power of proton beam will be upgraded to 240 kW and a second target station consisting of two targets in tandem to produce muons and white neutrons has been proposed in CSNS Phase II. Fig. 1 shows a schematic view of CSNS layout with the location markers for the proposed muon facilities [2]. The tentative muon sources will be built in High Energy Proton Experiment Area (HEPEA) [3], where about 4% of the proton beam extracted from the Rapid Cycling Synchrotron (RCS) are to be injected by the method of halo scraping technique [4]. In HEPEA, four experimental areas for muon source facility, cloud chamber, photon radiography, radiation effects research, will share the proton beam in pulse-cutting mode or time-sharing mode.

Construction of high-flux muon sources is mainly based on high-flux proton accelerators, similar to the muon facilities in the following four organizations: ISIS in United Kingdom, J-PARC in Japan, PSI in Switzerland, and TRIUMF in Canada. Currently muon sources have been widely used in the fields of energy development, materials science, medical applications, as well as some fundamental scientific research on particle physics [5~8]. In HEPEA, the injected proton beam has the power of 4.8 kW (Phase I), 90% of which will be used to bombard the muon target. According to the experience of international muon facility construction, there are many notable advantages associated with surface muon beams: high available muon beam flux; high longitudinal spin polarization (~100%); small beam spots; short beam line and low cost. We have long devoted to the study of the surface muon facility in CSNS, and some preliminary simulation results and conceptual design for muon target and transport beam line are given in this article.

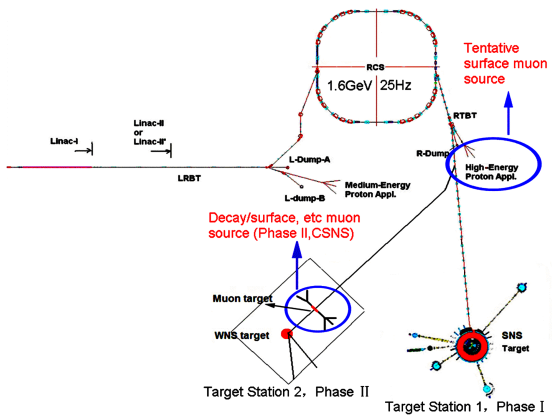

Fig.1 Layout of CSNS and muon source (color online)

2 Conceptual design and simulation research

By Monte Carlo simulation and particle beam transport matrix calculation, physical processes were simulated and studied. In this way, the following param-

*supported by National Natural Science Foundation of China (No. 11075154)

eters of muon source construction are given: parameters of muon target, production ratio of surface muons, muon beam flux, angular divergence, beam spot size and phase space distribution, all them are valuable for feasibility analysis on the muon source construction.

2.1 Simulation and design of muon target

The surface muon production is a process in which the proton beams bombard the solid target to produce the pion mesons, of which the low kinetic energy ones stop near the target surface and soon (~2.6 ns) decay into 4 MeV (momentum of 29.8 MeV/c) muons with an isotropic distribution. Then these muons are captured, transported, and focused. In this process, muon target design is a significant step. In this section, Monte Carlo simulation codes such as Geant4 [9] and Fluka [10] are employed to study the muon target design.

The characteristics of proton beams used in simulation are energy (1.6 GeV), energy spread (~0.3%), Gaussian function of particles distribution in space ($\sigma_{X/Y} = 3$ mm), beam emission (0), Gauss time structure ($\sigma_T = 18$ ns), repetition frequency (1 Hz, 2 bundles/pulse), and beam flux (1.92×10^{13} /pps). Fig. 2 shows the production ratios of various secondary particles as a function of momentum in a 4π solid angle of muon target. In this Geant4 simulation, a graphite muon target with thickness of 80 mm, radius of 15 mm was chosen. As we can see from Fig. 2, the positive muon yield curve reaches a peak at about 30 MeV/c, with sharp decrease by $P^{3.5}$ when the momentum decreases to below 30 MeV/c. These simulation results of production ratio roughly fit the experimental measurement results at TRIUMF [11].

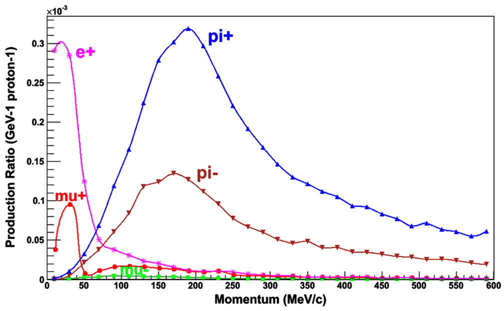

Fig.2 Production ratio of secondly particles for a graphite target of 15 mm in height and 80 mm in length (color online)

It is more flexible for us to design muon target than other muon facilities because it is unnecessary to consider performance of proton beam after bombarding the target at our facility. With the aims at high secondary particle yield-ratio and quick target cooling of kW-level power deposition generated by proton beam, we select solid muon targets with good thermal conductivity, small thermal expansion coefficient, fast thermal conductivities, large Young's modulus, and low Poisson's ratio, such as low Z material (graphite, beryllium) and high Z material (tantalum and tungsten). Our simulation of proton beam intensity and energy spectrum after bombarding the target and Ref. [11] shows that both the low-Z and high-Z materials can be used as the muon target for CSNS tentative muon facility. Finally, the proton beam power used for muon production can be expected to have a maximum value of 2.6 kW (~55% of the primary beam power of 4.8 kW), while a thickness of 80 mm is chosen for high-Z target.

Before escaping, decaying muons go through a long distance from pions stop in target to target surface. There are so many muons stopping and decaying in the target that the target radius must be carefully studied in the target design, with the initial proton beam spot size and the range of surface muons in solid materials taken into consideration. The muon yield ratios from target surface as a function of target radius for four different targets in 80 mm thickness were calculated using Geant4 and Fluka (Fig. 3 and Fig. 4), respectively. The momentum spread of surface muons is 25~30 MeV/c. The production ratio of surface muons from high Z target descends sharply as the radius increases, while the yield for low Z target changes relatively gently. To some extent, it has generally a significant relationship to the range (R) and range straggling (ΔR) of muon in materials. The range and range straggling of surface muon vary with the momentum as follow:

$$R = aP^{3.5}, \tag{1}$$

$$\Delta R = 3.5(\Delta P/P)P^{2.5}, \tag{2}$$

where P is the muon momentum and a is a constant that depends upon the materials. The range and the range straggling of the surface muons (~29.8 MeV/c) are 150 mg/cm^2 and 30 mg/cm^2 [12], respectively. The range values in millimeter for the four materials are C (0.7 mm/0.14 mm), Be (0.8 mm/0.16 mm), Ta (0.09 mm/0.018 mm) and W (0.078 mm/0.016 mm), which are much thinner than the radius of the target. It is indeed fairly thin because of the extremely small range and range straggling that a great quantity of positive muons will be absorbed within a small volume around their production position. While the target radius increases, most low momentum muons go to stop and decay in the target, especially in high-Z targets. In addition, both the Geant4 and Fluka results show that the muons yield ratio curves have an approximately periodic fluctuation in a small range of target radius, which is also due to the small range and range straggling of the surface muon.

The above studies come to a conclusion that we could consider thick solid materials with high-Z and high density as the muon target for different projects of CSNS tentative muon source. The utilization of proton beams can reach as high as 2.6 kW (W target, 80 mm thick). For achieving the maximum muon yield, it is optimal to use a ~7 mm thick Ta or ~5 mm thick W as the muon target for a proton beam with 20 mm spot size in diameter. For low-Z targets, the optimal target radius must be larger than the beam spot size (C: ~17 mm, Be: ~15 mm). Most surface muons are produced near the central area of the muon target with an outlet direction mainly perpendicular to the target cylinder axis. Therefore, the axis of the muon capture system will be designed to be perpendicular to the direction of the original proton beam and intersect the proton beamline at the center of muon target.

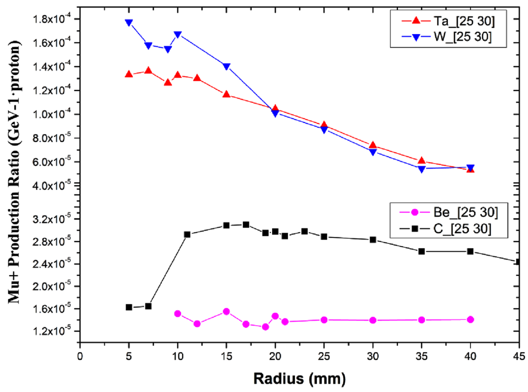

Fig.3 Surface muon production ratio vs. target radius for a graphite target of 80 mm in length: result using Geant4 (color online)

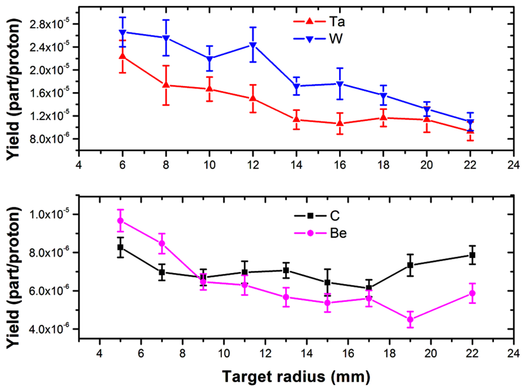

Fig.4 Surface muon production ratio vs. target radius for a graphite target of 80 mm in length: result using Fluka (color online)

2.2 The simulation and design of muons transport

Owing to the high radiation in the vicinity of muon target, the surface muon must be transported away from the target. A sequence of elements for beam optics should be installed for double focusing, particle bending and particle separating. Referred to the earliest construction experience of surface muon facilities [13], a simple beam transport line has been designed for CSNS tentative muon source (Fig. 5). In this system, sector bending magnets, quadruple magnets and a separator are used. The Q1-B1-Q2 triplet (Q, B represented as quadruple magnet and bending magnet, respectively) images the beam spot at target on the centre of Q2. The back half section of this system (B2, Q3-B3-Q4) will finally image the beam spot on the experiment area. System Q2-B2-Q3 adopts symmetrical beam optics between B2 and B3.

In this article, optical beam matrix calculation tools such as TRANSPORT [14] and TURTLE [15] were used. At first, the initialization parameters for simulation between the target and the first instrument of beamline were set as follows: the distance is 0.5 m, bending magnet provides a 30° bend, gaps of quadruple and bending magnet for capturing the surface muon are 400 mm and 500 mm, respectively. In this condition, the calculated solid angle acceptance is 450 mSr. Table 1 shows the calculated parameters of all elements in the system. With the above parameters, the envelopes of the surface muon in the horizontal and vertical planes were showed in Fig. 6. The overall length of the transport beamline is 6.5 m. The curves closer to the horizontal axis are the envelopes calculated in the first order optics, differing from the outside curves obtained in the second-order magnetic field calculation. From the first-order calculated result, it is found that the surface muon beam could well be transported from target to experiment area using this simple transport system, but the second-order envelope has a big divergence in the later half section, especially in the vertical plane, because it is difficult to realize a symmetrical layout. With different target thickness, the flux will vary in the range of $5\times10^4 \sim 10\times10^4$. As to the flux obtained for different target materials, the ratio of the flux for graphite to that for other materials is similar to the muon production ratio shown in Fig. 3.

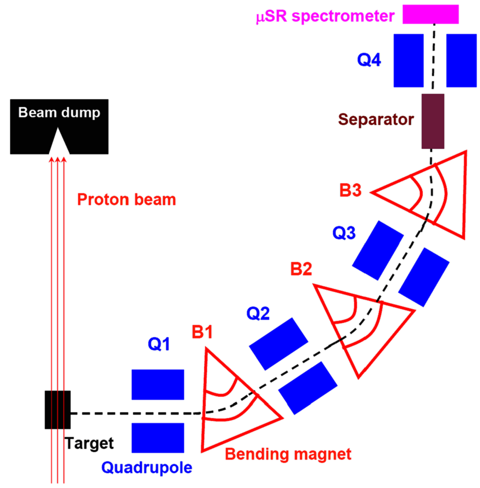

Fig.5 Layout of the simple surface muon beamline

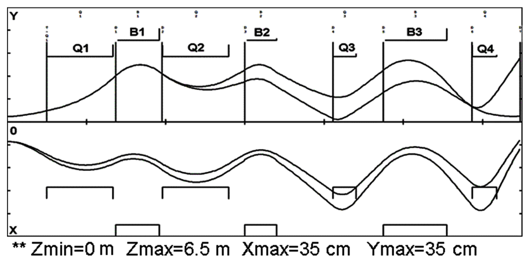

Fig.6 Horizontal and vertical envelopes for the surface muon beam in transport system

To sum up, there are some shortcomings in this simple muon facility design. It has an imperfect performance of muon beam optics in beam focusing, which shows the beam envelope of second order magnetic field simulation is not in accord with the one of first order.

Table 1. Effective length and magnetic field for quadruple and bending magnet

	Quadruple magnet				Bending magnet		
	Q1	Q2	Q3	Q4	B1	B2	B3
Effective length, $L_{\rm eff}$ (m)	0.8355	0.8355	0.2956	0.3079	0.55	0.40	0.8
Magnetic field, B (kG)	0.4805	0.4805	1.1826	1.8505	0.8733	1.2008	0.6004

Table 2. The characteristics of several pulse muon source facilities

Parameter	ISIS	J-PARC (Phase I)	CSNS-II	Tentative muon in CSNS
Proton Energy (GeV)	0.8	3.0	1.6	1.6
Current (A)	200	333	38	3
Primary (Loss in target) (kW)	160/4.8	120/7.8	60/3	4.8/2.5
Repetition rate (Hz)	50	25	12.5	1
Bunches per pulse	2	2	1	2
Carbon target thickness (mm)	10	20	20	40∼80
Muon line acceptance (mSr)	30	40	40	100∼200
Surface muon intensity (μ^+/s)	6×10^5	3×10^7	1.2×10^6	$1\times10^5\sim5\times10^5$
Decay muon intensity (μ^-/s)	$10^{4\sim5}$	$10^{6\sim7}$	$10^{5\sim6}$	–

Furthermore, the optimal parameters of all elements in the transport beamline will be retrieved with careful consideration regarding target design and SR experimental area design. In addition, we will use triplet quadruple magnets (consisting of 3 lenses), which can achieve perfect horizontal and vertical focusing in beam optics instead of a single quadruple magnet. In a complex transport beam line system, collimation elements are needed to control the beam momentum broadening, spot size, angular divergence and so forth.

The expected characteristics of tentative surface are given in Table 2 with a comparison to other pulse muon source facilities.

3 Summary

In this paper, the simulations of a surface muon facility, including muon target design and surface muon beamline design, are based on the proton beam characteristics used for HEPEA on CSNS. In order to obtain effective surface muon source, we carried out a detailed simulation to find the optimal parameters for target structure, selected appropriate material for solid target and designed elements for beam optics. Conclusions can be made as follow: The optimal surface muon yield may reach $10^{-5}\sim10^{-6}$ proton$^{-1}\cdot$GeV^{-1} when targets with thickness of 80 mm and radius of 17 mm (C), 15 mm (Be), 7 mm (Ta), and 5 mm (W) are used; the final surface muon performance can achieve a flux of 10^5 /s, a beam spot size of 5 cm×3 cm and a momentum spread of less than 10%. In summary, the proposed tentative muon facility at CSNS plans to include a high power muon production target station, a muon capture system, a 5∼10 m long muon beam transport line, a sample chamber for muon experiment, a complex system for μSR spectrometer and data acquisition. With the support of National Natural Science Foundation of China, our research group are now devoting ourselves to the design of the first muon source in China.

References

1 Wei J, Chen H S, Chen Y W, et al. 2009, Nuclear Instruments and Methods in Physics Research A, 600: 10
2 Wang S, Fang S X, Fu S N, et al. 2009, Chinese Physics C, 33 (Suppl. II): 1
3 Tang J Y, Li J C, Jing H T, et al. 2009, Consideration of applications for intermediate energy proton beam, white neutron source, and muon source using CSNS-I proton beam. Presented at 2009 CSNS Multi-application Symposium, Beijing, China, November 18-20 (in Chinese)
4 Tang J Y, Wei G H, Zhang C, et al. 2008, Beam preparation for injection into the CSNS RCS (R). Presented at 42nd ICFA Advanced Beam Dynamics Workshop on High-Intensity, High-Brightness Hadron Beams. Nashville, Tennessee, USA, August 25-29, 2008
5 Bandyopadhyay A, Choubey S, Gandhi R, et al. 2009, Rep. Prog. Phys., 72: 10
6 Jones S E. 1986, Nature, 321: 127
7 Bogdanova L N, Bom V R, Demin A M, et al. 2009, Journal of Experimental and Theoretical Physics, 108: 216
8 Blundell S J. 1999, Contemporary Physics, 40: 175
9 Geant4 - http://geant4.cern.ch
10 Fluka - http://www.fluka.org
11 Oram C J, Warren J B, Marshall G M, et al. 1981, Nuclear Instruments and Methods, 179: 95
12 Brewer J H. 1981, Hyperfine Interactions, 8: 831
13 Pifer A E, Bowen T, Kendall K R. 1976, Nuclear Instruments and Methods, 135: 39
14 PSI Graphic Transport Framework by U. Rohrer based on a CERN-SLAC-FERMILAB version by K.L. Brown et al.
15 PSI Graphic Turtle Framework by U. Rohrer based on a CERN-SLAC-FERMILAB version by K.L. Brown et al.

(Manuscript received 17 May 2011)
(Manuscript accepted 18 July 2011)
E-mail address of correspongding author
YE Bangjiao: bjye@ustc.edu.cn